An introduction to the Statistical Hadronization Model

Francesco Becattini
Università di Firenze and INFN Sezione di Firenze,
Via G. Sansone 1, I-50019, Sesto Fiorentino (Firenze), Italy
becattini@fi.infn.it

Abstract

In these lectures I review the foundations and the applications of the statistical hadronization model to elementary and relativistic heavy ion collisions. The role of strangeness production and the general interpretation of results is addressed.

Lectures given at the 4th edition of the school
Quark-Gluon Plasma and Heavy Ion Collisions : past, present, future
Torino (Italy), 8-14 December 2008

1 Introduction

A major phenomenon that the theory of strong interactions, quantum chromodynamics (QCD), should account for is confinement: quarks and gluons are not observable particles. In fact, every physical process involving strong interactions at high energy results in the formation of hadrons, in which quarks and gluons are confined on a distance scale of $\mathcal{O}(1)$ fm. While, up to now, there is no formal proof that QCD implies confinement, there are many indications, both from perturbative and from lattice numerical studies, that this is likely the case. Perturbative QCD is applicable to scattering processes of quarks and gluons involving large momentum transfer ($\gg 1$ GeV) because the strong coupling constant α_S is small enough to allow a series expansion. However, this is no longer possible at a scale of 1 GeV or below, where the perturbative expansion is meaningless, and where confinement and hadronization, the process of hadron formation, takes place. Thus, hadronization is not yet calculable from QCD first principles and one has to resort to phenomenological models. While this may seem an inconvenient limitation, still much can be learned from these models about QCD in the confinement regime. Indeed, if they are able to effectively describe the essential features of the actual physical process, they give us relevant information about the characteristics of the fundamental theory.

In these lectures, we will review a model with a rather long history, that has recently been revived by its successes in the description of hadronic multiplicities both in high energy elementary collisions and relativistic heavy ion collisions: the Statistical Hadronization Model (SHM).

2 The statistical hadronization model

The idea of applying statistical concepts to the problem of multi-particle production in high energy collisions dates back to a work of Fermi [1] in 1950, who assumed that particles originated from an excited region evenly occupying all available phase space states. This was one of Fermi's favorite ideas and soon led to an intense effort in trying to work out the predictions of inclusive particle rates calculating, analytically and numerically, the involved multidimensional phase-space integrals. When it became clear that the (quasi) isotropic particle emission in the center-of-mass frame predicted by Fermi's model was ruled out by the data, an amendment was put forward by Hagedorn [2] in the '60s, who postulated the existence of two hadron emitting sources flying apart longitudinally in the center-of-mass frame of a pp collision. Thereby, one could explain the striking difference between spectra in transverse and longitudinal momentum. Hagedorn was also able to explain the almost universal slope of p_T spectra in his renowned statistical bootstrap model, assuming that resonances are made of hadrons and resonances in turn.

After QCD turned up, many phenomenological models of strong interactions were no longer pursued and the statistical model was no exception. The resurgence of interest in these ideas came about when it was argued that a completely equilibrated hadron

gas would be a clear signature of the formation of a transient Quark-Gluon Plasma (QGP) in heavy ion collisions at high energy. While it has been indeed confirmed that an (almost) fully equilibrated hadron gas has been produced [3] in those collisions, the interest in this model was also revived by the unexpected observation that it is able to accurately reproduce particle multiplicities in elementary collisions [4]. Naively, one did not expect a statistical approach to work in an environment where the number of particles is $\mathcal{O}(10)$ because it was a belief of many that a hadronic thermalization process would take a long time if driven by hadronic collisions. Apparently this is not the case and one of the burning questions, which is still waiting a generally accepted answer, is why a supposedly non-thermal system exhibits a striking thermal behavior.

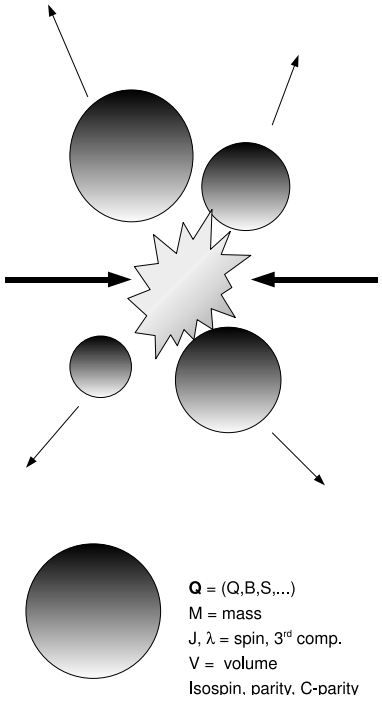

Figure 1: High energy collisions are assumed to give rise to multiple clusters at the hadronization stage [top]. Each cluster [bottom] is a colorless extended massive object endowed with abelian charges (electric, strange, baryonic etc.), intrinsic angular momentum and other quantum numbers such as parity, C-parity and isospin.

Before we address this interesting issue, it is appropriate to provide a rigorous formulation of the model in a modern form, which is necessarily different from Fermi's original model due to the tremendous improvement in our knowledge of strong interactions phenomenology. The Statistical Hadronization Model (SHM) must be considered as an effective model describing the process of hadron formation in high energy collisions at energy (or distance) scales where perturbative QCD is no longer applicable. A high energy collision is thought of as a complex dynamical process, governed by QCD, which

eventually gives rise to the formation of extended massive colorless objects defined as *clusters* or *fireballs* (see Fig. 1). While the multiplicity, masses, momenta and charges of these objects are determined by this complex dynamical process, the SHM postulates that hadrons are formed from the decay of each cluster in a purely statistical fashion, that is:

> *Every multihadronic state localized within the cluster and compatible with conservation laws is equally likely.*

This is the *urprinzip* of the SHM. The assumption of the eventual formation of massive colorless clusters is common for many hadronization models (e.g. the cluster model implemented in the Monte-Carlo code HERWIG [5]) based on the property of color preconfinement [6] exhibited by perturbative QCD. The distinctive feature of the SHM is that clusters have a finite spacial size. This aspect of clusters as a relativistic massive extended objects coincides with that of a bag in the MIT bag model [7]. Indeed, the SHM can be considered as an effective model to calculate bag decays.

The requirement of finite spacial extension is crucial. If the SHM is to be an effective representation of the QCD-driven dynamical hadronization process, this characteristic must be ultimately related to the QCD fundamental scale $\Lambda_{\rm QCD}$. As we will see, the universal soft scale shows up in the approximately constant energy density at hadronization; in other words, the volume of clusters is in a constant ratio with their mass when hadronization takes place. It is also worth stressing here that there is clear, independent evidence of the finite size of hadronic sources in high energy collisions. Quantum interference effects in the production of identical particles, the so-called Bose-Einstein correlations or Hanbury Brown-Twiss second-order interference, is by now a firmly established phenomenon. This effect would simply be impossible without a finite volume.

3 Localized states

The basic postulate of the Statistical Hadronization Model asserts that every localized multihadronic state which is contained within a cluster and is compatible with conservation laws is equally likely. The word *localized*, implying a finite spacial size, plays a crucial role, as we have emphasized. Thus, before getting to the heart of the SHM formalism, it is necessary to pause and clarify the distinction between localized and asymptotic states.

Such a difference is not an issue when the volume is sufficiently larger than the Compton wavelength of hadrons and it is disregarded in most applications where clusters supposedly meet this requirement (e.g. heavy ion collisions); yet, it is an important point at a fundamental level. Although in thermodynamics the focus is on the limit of infinite volumes, we must start from a finite volume and localized systems to introduce concepts like energy density, temperature etc. Furthermore, in the hadronic world, finite size effects must be diligently taken into account when the volume is comparable to the (third power of) the pion's Compton wavelength, ~ 1.4 fm.

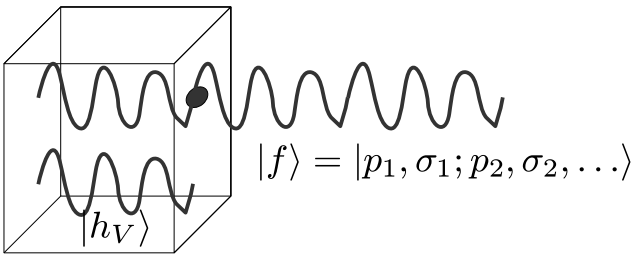

Figure 2: The localized multi-hadronic states $|h_V\rangle$ pertaining to the quantum field problem in a limited region. Asymptotic states $|f\rangle$ are the usual free states characterized by particle momenta and spin components.

The difference between a localized and an asymptotic state is depicted in Fig. 2. For a single particle in a Non-Relativistic Quantum Mechanics (NRQM) framework, the conceptual difference is easier to grasp: a localized state is described by a wavefunction which vanishes outside the cluster's region whereas an asymptotic state is a wavefunction which is defined over the whole space (e.g. a plane or a spherical wave). In Quantum Field Theory (QFT), a localized state is a state of the Hilbert space defined by the localized problem, e.g. the problem of the quantum field in the cluster's finite region. For a free field, if we enforce fixed or periodic boundary conditions, such states are simply defined by integer occupation numbers for each allowed mode in the finite region, as is well known. For a multiparticle state of non-interacting hadrons, this state will be defined by all occupation numbers of the modes determined by the fields associated with the different species of hadrons, and we will simply denote it with $|h_V\rangle$ (where h stands for "hadrons" and V stands for the finite region of volume V). On the other hand, an asymptotic state is a state of the Hilbert space defined by the quantum field operators over the whole space; for a free field, these are the familiar multi-particle free states defined by, e.g., momentum and polarization:

$$|f\rangle = |p_1, \sigma_1, \ldots, p_N, \sigma_N\rangle \tag{1}$$

There is a noteworthy and deep difference between non-relativistic quantum mechanical and quantum field theoretical case. In the latter, particle number is not fixed and a localized state with multiplicity (defined as the sum of all occupation numbers) N does not necessarily correspond to an asymptotic state with particle multiplicity N[1]. Unlike in NRQM, a localized state with multiplicity N has non-vanishing projections over asymptotic states with different particle multiplicities. In symbols:

$$|N\rangle_V = \alpha_{0,N}|0\rangle + \alpha_{1,N}|1\rangle + \ldots + \alpha_{N,N}|N\rangle + \ldots \tag{2}$$

[1]We note that the multiplicity of an asymptotic free state is the properly defined number of particles

with the obvious condition that $\alpha_{i,N} \to 0$ when $V \to \infty$ for $i \neq N$. In particular, the vacuum of the finite-region problem $|0\rangle_V$ is different from the vacuum of the full-space problem $|0\rangle$, which is commonly known as the Casimir effect. With a straightforward mapping of the Hilbert space of the localized quantum field onto the full Hilbert space, it is possible to express destruction operators of the localized field as linear combinations of destruction *and* creation operators of the field defined over the whole space [8]. These relations would be sufficient to calculate the coefficients of the above equation, but this is not really needed in the SHM, as it will be soon clear.

4 The formalism: basics

Let us consider a cluster and assume first that it can be described as a *mixture* of states. Then, the basic postulate implies that the corresponding density matrix is a sum over all localized states projected onto the initial cluster's quantum numbers:

$$\hat{\rho} \propto \sum_{h_V} \mathsf{P}_i |h_V\rangle\langle h_V| \mathsf{P}_i \equiv \mathsf{P}_i \mathsf{P}_V \mathsf{P}_i \tag{3}$$

where $|h_V\rangle$ are multi-hadronic localized states and P_i is the projector onto the cluster's initial conserved quantities: energy-momentum, intrinsic angular momentum and its third component, parity and the generators of inner symmetries of strong interactions [2].

The operator P_i can be formally defined as the projector onto an irreducible vector of the full symmetry group and worked out in a group theory framework [9, 10]. It can be factorized into a "kinematic" projector, associated to general space-time symmetry, and a projector for inner symmetries. For the space-time symmetry, the relevant group is the extended orthochronous Poincaré group $\mathrm{IO}(1,3)^{\uparrow}$ and an irreducible state is defined by a four-momentum P, a spin J and its third component λ and a discrete parity quantum number $\pi = \pm 1$. Therefore:

$$\mathsf{P}_i = \mathsf{P}_{P,J,\lambda,\pi} \mathsf{P}_{inner} \tag{4}$$

If the projector $\mathsf{P}_{P,J,\lambda}$ is worked out in the cluster's rest frame where $P = (M, \mathbf{0})$, it further factorizes into the product of simpler projectors [9, 11], i.e.:

$$\mathsf{P}_{P,J,\lambda,\pi} = \delta^4(P - \hat{P}) \mathsf{P}_{J,\lambda} \frac{\mathsf{I} + \pi \hat{\Pi}}{2} \tag{5}$$

where $\hat{P}$ is the four-momentum operator, $\mathsf{P}_{J,\lambda}$ is a projector onto SU(2) irreducible states $|J, \lambda\rangle$ and $\hat{\Pi}$ is the space reflection operator.

As clusters are color singlets by definition, the projector P_{inner} involves flavor and baryon number conservation. In principle, the largest symmetry group one should consider is SU(3), plus three other U(1) groups for baryon number, charm and beauty

[2] Operators in the Hilbert space will be denoted with a hat. Exceptions to this rule are projectors, which will be written in serif font, i.e. P.

conservation. However, SU(3) symmetry is badly broken by the mass difference between strange and up, down quarks, so it is customary to take a reduced SU(2)⊗U(1) where SU(2) is associated with isospin and U(1) with strangeness. The isospin SU(2) symmetry is explicitly broken as well, but the breaking term is small and can generally be neglected. However, most calculations in the past have replaced isospin SU(2) with another U(1) group for electric charge, so that the symmetry scheme, from an original $\mathrm{SU}(2)_{isospin}\otimes\mathrm{U}(1)_{strangeness}\otimes\mathrm{U}(1)_{baryon}$ reduces to $\mathrm{U}(1)_{charge}\otimes\mathrm{U}(1)_{strangeness}\otimes\mathrm{U}(1)_{baryon}$.

Altogether, P_{inner} can be written as

$$\mathsf{P}_{inner} = \mathsf{P}_{I,I_3}\mathsf{P}_{\mathbf{Q}}\mathsf{P}_{\chi} \tag{6}$$

where I and I_3 are isospin and its third component, $\mathbf{Q} = (Q_1, \ldots, Q_M)$ is a vector of M integer abelian charges (baryon number, strangeness, etc.) and P_χ is the projector onto C-parity, which makes sense only if the system is completely neutral, i.e. $I = 0$ and $\mathbf{Q} = \mathbf{0}$; in this case, P_χ commutes with all other projectors.

From the density matrix (3) the probability of observing an asymptotic multiparticle state $|f\rangle$ is

$$p_f \propto \langle f|\mathsf{P}_i\mathsf{P}_V\mathsf{P}_i|f\rangle \tag{7}$$

which is well-defined in terms of positivity and conservation laws. In fact, (7) is manifestly positive definite and $p_f = 0$ if the state $|f\rangle$ has not the same quantum numbers as the initial state. By summing over all states $|f\rangle$, one obtains the trace of the operator $\mathsf{P}_i\mathsf{P}_V\mathsf{P}_i$ which is

$$\sum_f p_f \propto \mathrm{tr}(\mathsf{P}_i\mathsf{P}_V\mathsf{P}_i) = \mathrm{tr}(\mathsf{P}_i^2\mathsf{P}_V) = a\mathrm{tr}(\mathsf{P}_i\mathsf{P}_V)\,. \tag{8}$$

The constant a is divergent and positive. It can be directly checked by choosing the $|f\rangle$ as momentum eigenstates and using the expression on the right hand side of (5). The reason for its presence is the non-compactness of the Poincaré group, which makes it impossible to have a properly normalized projector. The last trace in (8) can be written as

$$\mathrm{tr}(\mathsf{P}_i\mathsf{P}_V) = \sum_{h_V}\langle h_V|\mathsf{P}_i|h_V\rangle \equiv \Omega \tag{9}$$

which is, by definition the *microcanonical partition function* [8], i.e. the sum over all localized states projected onto the conserved quantities defined by the selected initial state. If only energy and momentum conservation is enforced, Ω takes on a more familiar form:

$$\Omega = \sum_{h_V}\langle h_V|\delta^4(P - \hat{P})|h_V\rangle\,. \tag{10}$$

Although the mixture of states defined by Eq. (3) allows us to calculate probabilities of any measurement unambiguously, a cluster could in principle also be described by a pure quantum state. Actually, the mixture of states only expresses our ignorance about the true state of the system, which is in principle a pure one, or, more precisely, a pure state entangled with pure states of other clusters. To avoid slipping into fundamental

quantum mechanics problems of decoherence and measurement, we take a pragmatic stance here. It suffices to realize that in some low-energy collision events, only one cluster might be created whose state is then necessarily a pure one. According to the postulate of the SHM, this must be an even superposition of all localized states with the initial conserved quantities, i.e.

$$|\psi\rangle = \sum_{h_V} c_{h_V} \mathsf{P}_i |h_V\rangle \qquad \text{with } |c_{h_V}|^2 = \text{const}\,. \tag{11}$$

The probability of observing a final state $|f\rangle$ is then

$$\begin{aligned} |\langle f|\psi\rangle|^2 &= |\sum_{h_V} \langle f|\mathsf{P}_i|h_V\rangle c_{h_V}|^2 \qquad (12)\\ = \quad & \text{const} \sum_{h_V} |\langle f|\mathsf{P}_i|h_V\rangle|^2 + \sum_{h_V \neq h'_V} \langle f|\mathsf{P}_i|h_V\rangle\langle h'_V|\mathsf{P}_i|f\rangle c_{h_V} c^*_{h'_V}\,. \end{aligned}$$

If the coefficients c_{h_V} have random phases, the last term in Eq. (12) vanishes and we are left with the same expression appearing in Eq. (7); in other words an effective mixture description is recovered. Hence a new hypothesis is introduced in the SHM here: if the cluster is a pure state, the superposition of multi-hadronic localized states must have random phases.

Now the main goal of the model is to determine the probabilities (7) which involves the calculation of the projector $\mathsf{P}_V = \sum_{h_V} |h_V\rangle\langle h_V|$, a more limited task than the explicit calculation of all scalar products $\langle h_V|f\rangle$. Since the states $|h_V\rangle$ are a complete set of states of the Hilbert space H_V for the localized problem, the above projector is simply a resolution of the identity of the localized problem and can be written in the basis of the field states. For a real scalar field this is

$$\mathsf{P}_V = \int_V \mathcal{D}\psi |\psi\rangle\langle\psi| \tag{13}$$

where $|\psi\rangle \equiv \otimes_{\mathbf{x}} |\psi(\mathbf{x})\rangle$ and $\mathcal{D}\psi$ is the functional measure; the index V means that the functional integration must be performed over the field degrees of freedom in the region V, that is $\mathcal{D}\psi = \prod_{\mathbf{x}\in V} d\psi(\mathbf{x})$. One has to face several conceptual subtleties in the endeavor of calculating the probabilities (7) with the projector (13), e.g. how to deal with field boundary conditions and with their values outside the region V. However, by enforcing the known non-relativistic limit is possible to come to an unambiguous and consistent result [8].

5 Rates of multiparticle channels

According to the formulae introduced in the previous section, the decay rate of a cluster into a *channel* $\{N_j\}$ ($\{N_j\}$ is the array of multiplicities $(N_1, \ldots, N_K)$ for hadron species $1, \ldots, K$) is proportional to the right hand side of (7) integrated over momenta and

summed over polarization states of the final hadrons. Taking into account only energy-momentum conservation, so that the projector (5) reduces to

$$\mathsf{P}_{PJ\lambda\pi} \to \mathsf{P}_P = \delta^4(P - \hat{P})\,,$$

and neglecting quantum statistics effects, this is proportional to the microcanonical partition function with fixed particle multiplicities [9, 8]

$$\Omega_{\{N_j\}} = \frac{V^N}{(2\pi)^{3N}} \left(\prod_{j=1}^{K} \frac{(2S_j+1)^{N_j}}{N_j!} \right) \int d^3p_1 \ldots \int d^3p_N \; \delta^4(P_0 - \sum_i p_i) \langle 0|\mathsf{P}_V|0\rangle\,. \quad (14)$$

Here N is the number of particles, S_j the spin, $P_0 = (M, \mathbf{0})$, M is the mass and V is the cluster's proper volume. This formula is the same as it would be obtained in NRQM, with the factor $\langle 0|\mathsf{P}_V|0\rangle$ (which becomes 1 in the limit $V \to \infty$) being the only effect of the field theoretical treatment [8]. Since only relative rates make sense, this common factor for all channels is irrelevant.

Loosely speaking, Eq. (14) tells us that the decay rate of a massive cluster into some multi-hadronic channel is proportional to its phase space volume. However, it should be emphasized that the "phase space volume" in (14) is calculated with the measure $d^3x\, d^3p$ for each particle, and not with the one usually understood in QFT, i.e. $d^3p/2\varepsilon$. Although this is also commonly known as "phase space", it is quantitatively different from the properly called phase space measure $d^3x\, d^3p$ and should be called "invariant momentum space" measure [12].

Eq. (14) can be cast in a form which makes its Lorentz invariance apparent. Define a four-volume $\Upsilon = Vu$ [12] where V is the cluster's rest frame and u its four-velocity vector. Then (14) can be rewritten as:

$$\begin{aligned} \Omega_{\{N_j\}} = \quad & \frac{1}{(2\pi)^{3N}} \left(\prod_{j=1}^{K} \frac{(2S_j+1)^{N_j}}{N_j!} \right) \int d^4p_1 \ldots \int d^4p_N \\ & \left[\prod_{i=1}^{N} \Upsilon \cdot p_i \delta(p_i^2 - m_i^2)\theta(p_i^0) \right] \delta^4(P_0 - \sum_i p_i) \langle 0|\mathsf{P}_V|0\rangle \end{aligned} \quad (15)$$

which is manifestly covariant. In this form it can be directly compared with the general formula for the decay rate of a massive particle into a N-body channel:

$$\Gamma_N \propto \sum_{\sigma_1,\ldots,\sigma_N} \frac{1}{(2\pi)^{3N}} \left(\prod_j \frac{1}{N_j!} \right) \int \frac{d^3p_1}{2\varepsilon_1} \ldots \int \frac{d^3p_N}{2\varepsilon_N} \; |M_{fi}|^2 \delta^4(P_0 - \sum_i p_i) \quad (16)$$

where σ labels, as usual, polarization states. Comparing (14) with (16) we can infer a dynamical matrix element for the SHM which is

$$|M_{fi}|^2 \propto \prod_{i=1}^{N} \Upsilon \cdot p_i\,. \quad (17)$$

Therefore, according to the SHM the dynamics in cluster decay is limited to a common factor for each emitted particle, which linearly depends on the cluster's spacial size. The four-volume Υ is simply proportional to the four-momentum of the cluster through the inverse of energy density ρ and therefore:

$$|M_{fi}|^2 \propto \frac{1}{\rho^N} \prod_{i=1}^{N} P \cdot p_i \,. \tag{18}$$

This expression explicitly shows the separation between the kinematic arguments of the dynamical matrix element, and the scale $1/\rho$ which determines particle production. This ought to be ultimately related to the fundamental scale of quantum chromodynamics, $\Lambda_{\rm QCD}$.

It has already been stressed that the finite cluster size is the distinctive feature of the SHM. This peculiarity of the model stands out when taking into account quantum statistics for the calculation of decay rates. Our final result, for which (14) is a special case when all particles belong to different species, reads

$$\begin{aligned} \Omega_{\{N_j\}} &= \int d^3\mathrm{p}_1 \ldots d^3\mathrm{p}_N \; \delta^4(P_0 - \sum_{i=1}^{N} p_i) \prod_j \sum_{\{h_{n_j}\}} \frac{(\mp 1)^{N_j+H_j}(2S_j+1)^{H_j}}{\prod_{n_j=1}^{N_j} n_j^{h_{n_j}} h_{n_j}!} \\ &\times \prod_{l_j=1}^{H_j} F_{n_{l_j}} \; \langle 0|\mathsf{P}_V|0\rangle \end{aligned} \tag{19}$$

where $\{h_{n_j}\}$ is a *partition* of the integer N_j in the multiplicity representation, that is $\sum_{n_j=1}^{N_j} n_j h_{n_j} = N_j$, $\sum_{n_j=1}^{N_j} h_{n_j} = H_j$ and $\sum_j N_j = N$. The factor $F_{n_{l_j}}$ in Eq. (19) are Fourier integrals:

$$F_{n_l} = \prod_{i_l=1}^{n_l} \frac{1}{(2\pi)^3} \int_V d^3\mathrm{x} \; \mathrm{e}^{i\mathbf{x}\cdot(\mathbf{p}_{c_l(i_l)} - \mathbf{p}_{i_l})} \tag{20}$$

over the cluster's region V, c_l being a cyclic permutation of order n_l. The expression (19) has been obtained in refs. [9, 8] and is a generalization of a similar one calculated by Chaichian, Hagedorn and Hayashi [12] whose validity is restricted to large volumes. It is a so-called *cluster decomposition* of the microcanonical partition function of the channel. For sufficiently large volumes, all terms in Eq. (19) turn out to be proportional to the H_jth power of the volume V [9], so that the leading term is the one with $H_j = N_j$ for all j, which leads precisely to Eq. (14). Thus, Eq. (19) is a generalization of (14) containing all corrections due to quantum statistics.

In general, with respect to the Boltzmann case (14), the channel rate is enhanced by the presence of identical bosons and suppressed by that of fermions. This means that Bose-Einstein and Fermi-Dirac correlations are built into the SHM. The reader has probably anticipated this fact through the appearance of typical Fourier integrals in the cluster decomposition. This feature of the SHM is an almost obvious consequence of the cluster's finite spacial size.

6 Interactions

So far, we have dealt with non-interacting particles. However, the localized hadronic fields we have used to calculate transition probabilities do interact and this must be taken into account. The energy of the interacting system must be conserved until the final asymptotic multi-hadronic state is reached which is made of particles stable under strong interactions, namely pions, kaons, nucleons and octet hyperons.

Formally, this implies that the projector (5) must include the interacting Hamiltonian in the $\delta^4(P-\hat{P})$ operator[3]. The definition (7) for the probability to observe an asymptotic state $|f\rangle$, has to be modified by the insertion of Møller operator $\hat{\Omega}$, yet summing over the complete set of states yields the same result as in Eq. (8):

$$\sum_f p_f \propto \mathrm{tr}(\mathsf{P}_i \mathsf{P}_V \mathsf{P}_i) = a\,\mathrm{tr}(\mathsf{P}_i \mathsf{P}_V) = a \sum_{h_V} \langle h_V|\mathsf{P}_i|h_V\rangle \equiv a\,\Omega \tag{21}$$

where a is an irrelevant divergent constant and Ω is the microcanonical partition function of the interacting hadronic system.

An outstanding theorem by Dashen, Ma and Bernstein (DMB) [14] allows us to calculate the microcanonical partition function of an interacting system in the thermodynamic limit $V \to \infty$ as the sum of the free one plus a term depending only on the physical scattering matrix. It can be expressed as

$$\mathrm{tr}\delta^4(P-\hat{P}) = \mathrm{tr}\delta^4(P-\hat{P}_0) + \frac{1}{4\pi i}\mathrm{tr}\left[\delta^4(P-\hat{P}_0)\hat{\mathcal{S}}^{-1}\frac{\overleftrightarrow{\partial}}{\partial E}\hat{\mathcal{S}}\right] \tag{22}$$

where $\hat{P}$ includes the full interaction Hamiltonian, whereas $\hat{P}_0$ only contains the free one; $\mathcal{S}$ is the reduced scattering matrix on the energy-momentum shell. If more conserved quantities other than energy and momentum are involved, like those encountered in section 4, the theorem is readily extended and relevant projectors can be placed next to the δ-functions in Eq. (22); it suffices that these conserved quantities are associated with symmetries of both free and interacting theory.

This theorem is indeed the starting point of the *hadron-resonance gas* model since it can be shown that if only the resonant part of the scattering matrix is retained and the background interaction can be neglected, the main contribution of the second term on the right hand side of Eq. (22) is equivalent to considering all hadronic resonances as free particles with distributed mass. More specifically, if a cluster decomposition of the two scattering operators is carried out in Eq. (22), the corresponding diagrams can be divided in two sets: the symmetric diagrams (see Fig. 3, left panel) and the non-symmetric ones (see Fig. 3, right panel). Taking into account that the terminal legs on both sides have to be the same stable particles on entry and exit (we are calculating a trace), it can be shown that the main contribution to symmetric diagrams comes

[3]In all virtually known field theories, there is no additional interacting term for momentum and angular momentum [13].

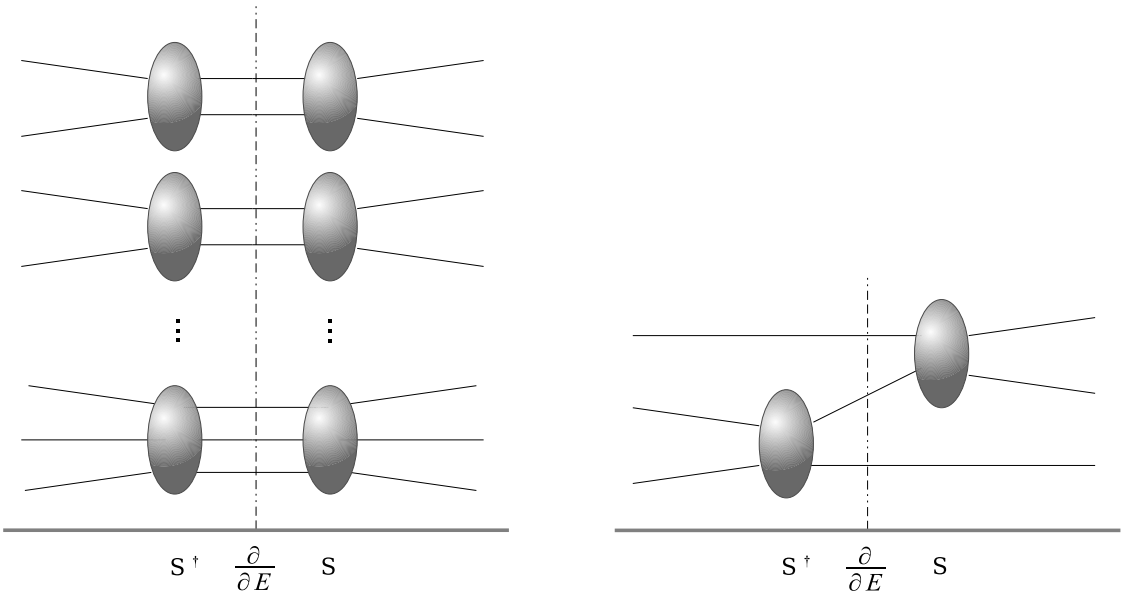

Figure 3: Left panel:symmetric diagrams for the cluster decomposition of the interaction term in the DMB theorem. Right panel: non-symmetric diagrams.

from the matching resonances in bubbles facing each other. For each term of the trace, this amounts to adding the decay products of resonances considered as free particles with masses distributed according to a relativistic Breit-Wigner form. In symmetric diagrams, there is in principle an additional contribution from resonance interference, which might be non-negligible in case of wide, overlapping resonances with the same decay channel, but it depends on mostly unknown complex parameters and it is thus neglected.

Likewise, the asymmetric diagrams give an additional contribution which also depends on the aforementioned complex interference parameters. While the number of such diagrams greatly exceeds the symmetric ones due to the large number of resonances, contributing terms can be both positive and negative and hopefully a partial cancellation occurs when summing them up for a selected final state.

Altogether, retaining only the resonant interaction and symmetric diagrams in the scattering matrix cluster decomposition, and neglecting resonance interference leads to the following picture: an interacting hadron gas is, to a good approximation, a gas of non-interacting free hadrons and resonances. Since non-resonant interaction should be negligible, the ideal hadron-resonance gas picture holds if the energy density or temperature of the system is large enough for most resonances to be excited. A quantitative assessment of how large these parameters are is still missing, a rough estimate being $T > 100$ MeV.

An important remark is now in order. The DMB theorem affirms the equality of two traces, but not of single trace terms. Yet, the decomposition of Eq. (22), implying the

ideal hadron-resonance gas picture, is widely used for the calculation of inclusive stable hadronic multiplicities as well, which requires a condition stronger than the equality of the traces on both sides. In other words, using the decomposition (22) to calculate average multiplicities or fluctuations requires the equality to hold for multiparticle generating functions and not only for microcanonical partition functions. Up to now, the extension of (22) to generating functions has never been proved; most likely, it does not hold and corrections to this assumption are necessary. Moreover, while the theorem requires the thermodynamic limit, it is commonly used at finite volume. These limitations should be always kept in mind when using the ideal hadron-resonance gas model.

7 High energy collisions

As we have seen in Sect. 5, each individual cluster produced in a high energy collision (shown in Fig. 1), should be hadronized according to formula (19), or its approximation (14), which yields the rates of a given channel within the microcanonical ensemble, including energy-momentum conservation. If clusters are large enough, the microcanonical ensemble could be well approximated by the canonical [9, 15] or even grand-canonical ensemble for average multiplicities. This is not the case in elementary collisions (e^+e^-, pp, etc.) while it is generally possible in heavy ion collisions, as we will see later in this section. Calculating observables in high energy collisions within the SHM then implies summing microcanonical averages over all produced clusters and this requires in turn knowledge of their charges and four-momenta. In fact, this latter information is unknown to the SHM and only a dynamical model of the pre-hadronization stage of the process (such as, e.g., HERWIG) can provide it.

However, if we are interested in calculating Lorentz-invariant observables (such as average multiplicities) the momenta of clusters are immaterial and only charges and masses matter. In this case, one can introduce a peculiar extra-assumption which allows to considerably simplify the calculation. Basically, it is assumed that the probability distribution:

$$w(\mathbf{Q_1}, M_1; \ldots, \mathbf{Q}_N, M_N)$$

of masses M and conserved abelian charges $\mathbf{Q}$ for N different clusters is the same as one would have by randomly splitting a large cluster (defined as *Equivalent Global Cluster*, EGC) into N subsystems with given volumes. Thereby, the Lorentz invariant observables can be calculated for one (equivalent global) cluster, whose volume is the sum of proper cluster volumes and whose charge is the sum of cluster charges, hence the conserved charge of the initial colliding system. The full mathematical procedure is described in detail in ref. [16].

In such a global averaging process, the EGC generally turns out to be large enough in mass and volume so that the canonical ensemble becomes a good approximation of the more fundamental microcanonical ensemble [15]; in other words, a temperature can be introduced which replaces the *a priori* more fundamental description in terms of energy density. It was shown that the mass of the EGC should be at least 8 GeV

(with an energy density of 0.5 GeV/fm^3) for the canonical ensemble to be a reasonably good approximation [15]. Also, it should be emphasized that in such a mathematical reduction process, temperature has essentially a global meaning and not local as in hydrodynamical models (see next subsection). The only meaningful local quantity in actual physical process are energy densities and individual physical clusters cannot be described in terms of a temperature, unless they are sufficiently large. Nevertheless, this "global" temperature closely mirrors the value of energy density at which clusters hadronize. Indeed, it is this latter value which mainly determines hadronization-related observables; the requirement of the charge distribution of EGC is a side-assumption which is important to simplify calculations, but it can possibly be replaced by other distributions leaving final results essentially unchanged.

In this approach, the primary multiplicity of each hadron species j is given by [16]:

$$\langle n_j \rangle^{\rm primary} = \frac{VT(2S_j+1)}{2\pi^2} \sum_{n=1}^{\infty} \gamma_S^{N_s n} (\mp 1)^{n+1} \, \frac{m_j^2}{n} \, {\rm K}_2\left(\frac{n m_j}{T}\right) \, \frac{Z(\mathbf{Q} - n\mathbf{q}_j)}{Z(\mathbf{Q})} \tag{23}$$

where V is the (mean) volume and T the temperature of the equivalent global cluster. Here $Z(\mathbf{Q})$ is the canonical partition function depending on the initial abelian charges $\mathbf{Q} = (Q, N, S, C, B)$, i.e., electric charge, baryon number, strangeness, charm and beauty, respectively; m_j and S_j are the mass and the spin of the hadron j, $\mathbf{q}_j = (Q_j, N_j, S_j, C_j, B_j)$ its corresponding charges; the upper sign applies to bosons and the lower sign to fermions.

The parameter γ_S in (23) is an extra phenomenological factor implementing an *ad hoc* suppression of hadrons with N_s strange valence quarks with respect to the equilibrium value. This parameter is outside a pure thermodynamical framework and it is needed to reproduce the data, as we will see. For temperature values of 160 MeV or higher, Boltzmann statistics, corresponding to the term $n = 1$ only in the series (23), is a very good approximation (within 1.5%) for all hadrons but pions. For resonances, the formula (23) is folded with a relativistic Breit-Wigner distribution for the mass m_j. The final multiplicities, to be compared with the data, are determined by adding to the primary multiplicity (23) the contribution from the decay of unstable heavier hadrons, according to the formula

$$\langle n_j \rangle = \langle n_i \rangle^{\rm primary} + \sum_k {\rm Br}(k \to j) \langle n_k \rangle \; . \tag{24}$$

The canonical partition function can be expressed as a multi-dimensional integral

$$\begin{aligned} Z(\mathbf{Q}) &= \frac{1}{(2\pi)^N} \int_{-\pi}^{+\pi} d^N\phi \; {\rm e}^{i\mathbf{Q}\cdot\boldsymbol{\phi}} \\ &\times \exp\left[\frac{V}{(2\pi)^3} \sum_j (2S_j+1) \int d^3p \; \log\left(1 \pm \gamma_s^{N_{sj}} {\rm e}^{-\sqrt{p^2+m_j^2}/T_i - i\mathbf{q}_j\cdot\phi}\right)^{\pm 1} \right] \end{aligned} \tag{25}$$

where N is the number of conserved abelian charges. Unlike the grand-canonical case, the logarithm of the canonical partition function does not scale linearly with the volume.

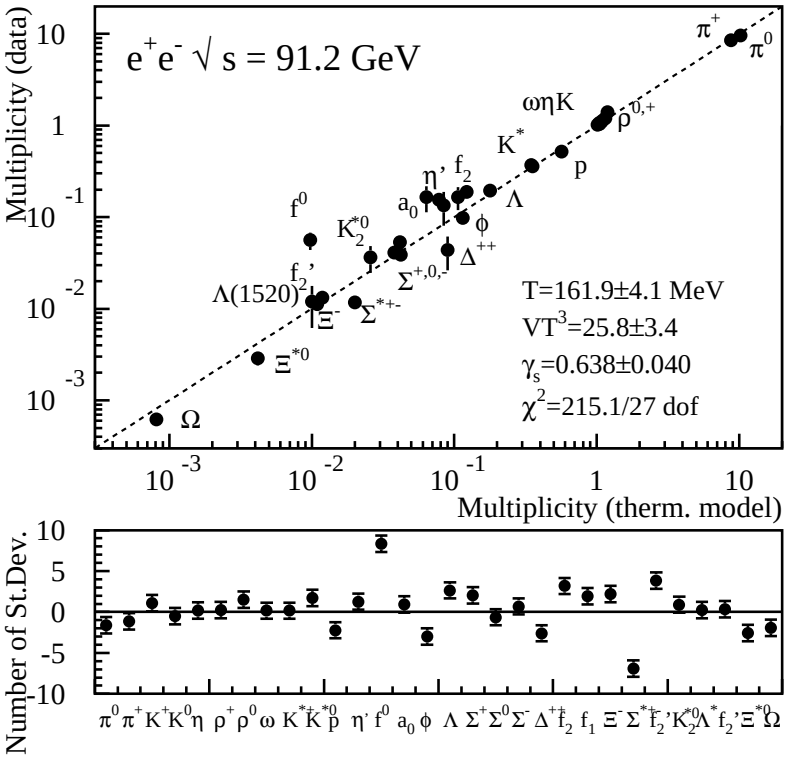

Figure 4: Upper panel: measured vs theoretical multiplicities of light-flavoured hadrons in e^+e^-collisions at $\sqrt{s} = 91.25$ GeV. Lower panel: fit residuals (from ref. [17]).

Therefore, the so-called *chemical factors* $Z(\mathbf{Q} - n\mathbf{q}_j)/Z(\mathbf{Q})$ [18] turn out to be less than unity even for a completely neutral system at finite volume (canonical suppression) and reach their grand-canonical value 1 at asymptotically large volumes [19, 4].

The light-flavoured multiplicities in e^+e^-show a very good agreement with the predictions of the model, as it shown in Fig. 4: the temperature value is about 160 MeV and the strangeness undersaturation parameter $\gamma_S \sim 0.7$. Similar good agreements are found for many kinds of high energy elementary collisions over a large energy range [4]. Also, an excellent agreement between measured and predicted relative abundances of heavy flavoured hadronic species in e^+e^-collisions by using the model parameters fitted to light-flavoured multiplicities [4, 17], as shown in Table 1.

The overall striking feature is that the temperature turns out to be approximately constant over two orders of magnitude in centre-of-mass energy with a value of 160-170 MeV (see Fig. 5) and very close to the QCD critical temperature as determined from lattice calculations. There must certainly be a profound connection between the thus-found hadronization temperature and QCD thermodynamics, a connection which

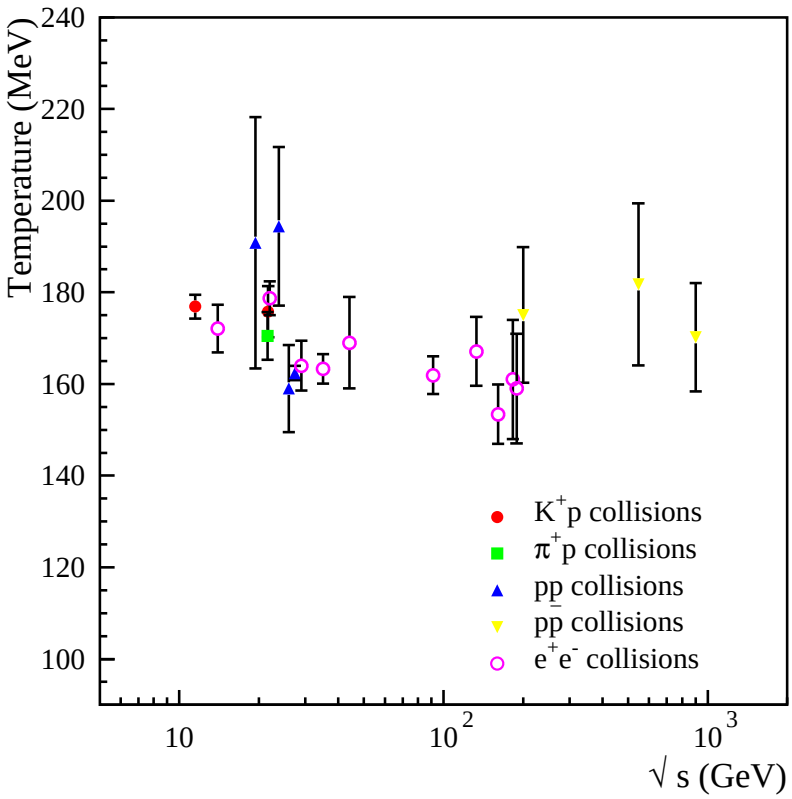

Figure 5: Temperatures fitted in elementary collisions as a function of center-of-mass energy.

has not been made clear yet. Nevertheless, this finding indicates that hadronization is a universal process occurring at a critical value of the local energy density, i.e. when clusters have an energy density of $\simeq 0.5$ GeV/fm^3.

The parameter γ_S is found to be less than 1 in all examined elementary collisions, ranging from ~ 0.5 in hadronic collisions to ~ 0.7 in e^+e^-collisions (see Fig. 10). This extra parameter most likely reflects the different mass of the strange quark with respect to lighter u, d quarks. This is a second scale, besides Λ_{QCD}, which must play a role in hadronization in view of its value $\mathcal{O}(100)$ MeV. Altogether, one can say that the SHM description of hadronization is in excellent agreement with QCD at least with regard to the the number of parameters. The two parameters T and γ_S correspond to the two fundamental scales Λ_{QCD} and m_s, the strange quark mass. While we lack a definite relation connecting them (see, however ref. [17]), it is worth stressing that a phenomenological description of hadronization in terms of fewer parameters cannot be possible.

Finally, the statistical model shows a very good capability of reproducing transverse

Particle	Experiment (E)	Model (M)	Residual	$(M-E)/E$ [%]
D^0	0.559 ±0.022	0.5406	-0.83	-3.2
D^+	0.238 ±0.024	0.2235	-0.60	-6.1
D^{*+}	0.2377±0.0098	0.2279	-1.00	-4.1
D^{*0}	0.218 ±0.071	0.2311	0.18	6.0
D_1^0	0.0173 ±0.0039	0.01830	0.26	5.8
D_2^{*0}	0.0484 ±0.0080	0.02489	-2.94	-48.6
D_s	0.116 ±0.036	0.1162	0.006	0.19
D_s^*	0.069 ±0.026	0.0674	-0.06	-2.4
D_{s1}	0.0106 ±0.0025	0.00575	-1.94	-45.7
D_{s2}^*	0.0140 ±0.0062	0.00778	-1.00	-44.5
Λ_c	0.079 ±0.022	0.0966	0.80	22.2
$(B^0+B^+)/2$	0.399 ±0.011	0.3971	-0.18	-0.49
B_s	0.098 ±0.012	0.1084	0.87	10.6
B^*/B(uds)	0.749 ±0.040	0.6943	-1.37	-7.3
$B^{**} \times BR(B(^*)\pi)$	0.180 ±0.025	0.1319	-1.92	-26.7
$(B_2^* + B_1) \times BR(B(^*)\pi)$	0.090 ±0.018	0.0800	-0.57	-11.4
$B_{s2}^* \times BR(BK)$	0.0093 ±0.0024	0.00631	-1.24	-32.1
b-baryon	0.103 ±0.018	0.09751	-0.30	-5.3
Ξ_b^-	0.011 ±0.006	0.00944	-0.26	-14.2

Table 1: Abundances of charmed hadrons in $e^+e^- \to c\bar{c}$ annihilations and bottomed hadrons in $e^+e^- \to b\bar{b}$ annihilations at $\sqrt{s} = 91.25$ GeV, compared to the prediction of the statistical model (from ref. [17]).

momentum spectra in hadronic [16] as well as heavy ion collisions [20] (see fig. 6). Particularly, the phenomenon of approximate m_T scaling observed in pp collisions is nicely accounted for by the model. However, the exact $\mathbf{p}_T$ conservation at low energy and the increasing importance of jet emission at high energy restrict the validity of the statistical canonical formulae to a limited centre-of-mass energy range. Within this region, a clear consistency is found between the temperature parameter extracted from the spectra and that from average multiplicities. Altogether, this finding bears out one of the key predictions of the SHM, namely the existence of a definite relation between the dependence of particle production rates on mass and, for each particle species, their momentum spectra (in the cluster's rest frame) because they are both governed by one parameter, the energy density (or temperature) at hadronization.

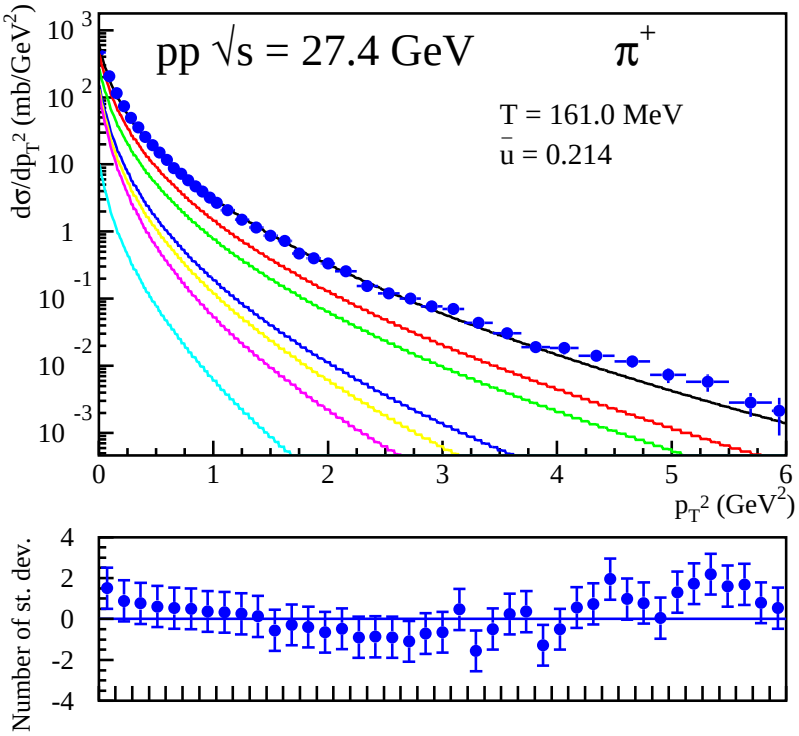

Figure 6: Transverse momentum spectrum of π^+ in pp collisions at $\sqrt{s}$ = 27 GeV (from ref. [16]). Full dots are data from experiment NA27; the black line is a fit with temperature T=161 MeV and average transverse four-velocity of hadronizing clusters ~ 0.21. Coloured lines show the cumulative contribution of resonance decays, divided into classes according to their quantum numbers.

8 Heavy ion collisions

In heavy ion collisions, the system is much larger and two possibilities are usually envisaged: either hadronizing clusters are simply much larger than those in elementary collisions; or clusters are hydrodynamical cells, i.e. they are small but in thermal contact with each other due to previous thermalization, which implies a strong correlation between their position and momentum and charge densities (see Fig. 7). In both case the canonical or grand-canonical formalisms apply to individual clusters. For the former case, it is worth mentioning that the transition from a canonical to a grand-canonical description effectively occurs when the cluster volume is of the order of 100 fm^3 at an energy density of 0.5 GeV/fm^3 [18]. If the EGC reduction assumption still applies, chemical factors in Eq. (23) are replaced by fugacities, and in this case the phase-space

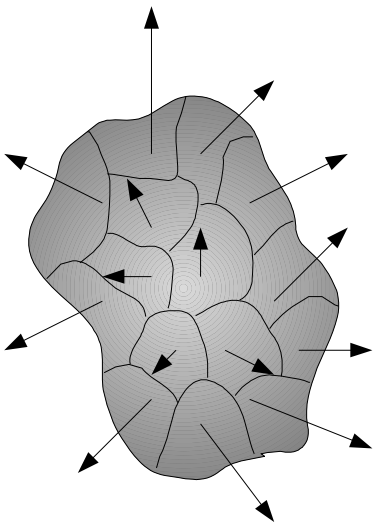

Figure 7: Spacial distributions of clusters in heavy ion collisions according to the hydrodynamical picture. In this model, nearby clusters interact from an early stage on and their momenta and charges are strongly correlated with their positions, unlike in elementary collisions.

integrated multiplicities read

$$\langle n_j \rangle^{\text{primary}} = \frac{VT(2S_j+1)}{2\pi^2} \sum_{n=1}^{\infty} \gamma_S^{N_s n} (\mp 1)^{n+1} \, \frac{m_j^2}{n} \, \mathrm{K}_2\left(\frac{n m_j}{T}\right) \exp[n\boldsymbol{\mu} \cdot \mathbf{q}_j / T] \,. \qquad (26)$$

$\boldsymbol{\mu}$ is a vector of chemical potentials pertaining to the conserved abelian charges, i.e. the electrical chemical potential μ_Q, the baryon chemical potential μ_B and the strangeness chemical potential μ_S. Usually, but not always, μ_S and μ_Q are determined by enforcing strangeness neutrality and by fixing the ratio Q/B to be the same as the initial Z/A ratio of the colliding nuclei.

In the framework of the hydrodynamical model, formula (26) applies to individual clusters identified with hydrodynamic cells and both temperature and chemical potentials depend on space-time; when integrating particle densities to get average multiplicities, one should take into account this dependence. It is important to stress that the hydrodynamical description is a salient feature of heavy ion collisions due to the early thermalization of the system in the partonic phase, a phenomenon which does not occur in elementary collisions. It is this early thermalization which establishes the strong correlation between positions and velocities of clusters, supposedly absent in elementary collisions.

Provided that rapidity distributions are wide enough, and that there is little variation of the thermodynamical parameters of clusters around midrapidity, the formula (26) describes rapidity densities of hadrons at midrapidity as well: this condition is fulfilled at RHIC energies, but not at AGS and SPS energies, where the measured rapidity

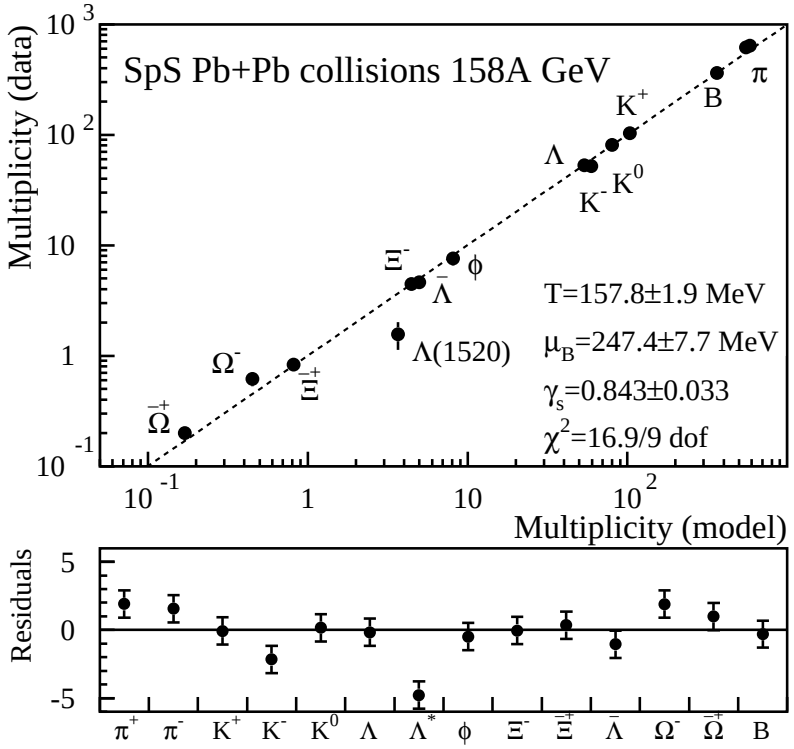

Figure 8: Upper panel: measured vs theoretical multiplicities of light-flavoured hadrons in Pb-Pb collisions at $\sqrt{s}_{NN} = 17.2$ GeV. Lower panel: fit residuals (from ref. [21]).

distributions are not significantly wider than those of a single fireball at the temperature found [22].

In general, the fits to particle multiplicities in heavy ion collisions are of the same good quality as in elementary collisions (see Fig. 8). Many groups have analyzed the data over more than a decade [3] and the overall description is very good throughout all explored energies and one finds a smooth curve in the $T - \mu_B$ plane (see Fig. 9).

9 Strangeness production

The statistical model is a very useful tool to study one of the main features of relativistic heavy-ion collisions, the increase of relative strangeness production with respect to elementary collisions. This was one of the early signatures proposed for Quark-Gluon Plasma formation [24], and it has therefor attracted much attention both on the theoretical and experimental side. According to the SHM, this is mainly an effect of the increase

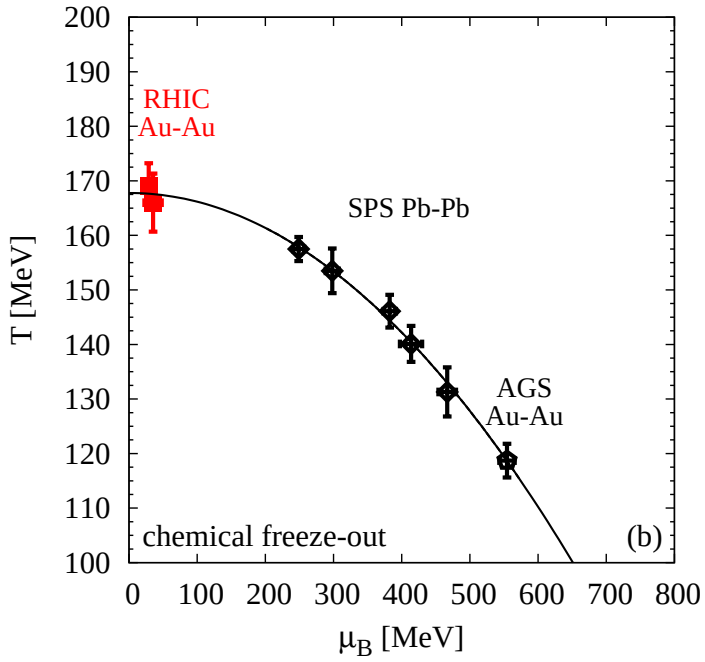

Figure 9: Temperature vs baryon chemical potential fitted with multiplicities in heavy ion collisions (from ref. [23]).

of the global volume from elementary to heavy-ion collisions. In elementary collisions, the EGC volume is small enough for the chemical factors (see Eq. (25)) of strange particles to be consistently less than 1 for systems with vanishing net strangeness, a phenomenon known as strangeness canonical suppression.

However, canonical suppression is not enough to account for strangeness enhancement from pp to heavy-ion collisions: also an increase of γ_S is needed. This is demonstrated by neutral mesons containing strange quarks, especially ϕ meson, which do not suffer canonical suppression but are relatively more abundant in heavy-ion collisions [25, 26]. Therefore, from a SHM viewpoint, one can say that, as far as particle abundances is concerned, the only substantial difference between elementary and heavy ion collisions resides in the different γ_S values, which are generally higher in heavy-ion collisions and increase slowly as a function of center-of-mass energy (see Fig. 10): at RHIC energies one finds $\gamma_S \simeq 1$ in central collisions. However, since γ_S is an empirical parameter which lies outside of a pure statistical mechanics framework, this observation does not clarify the origin of strangeness enhancement.

It is interesting to note that, while γ_S shows no special regularity in elementary collisions, the ratio of newly produced $\bar{\mathrm{s}}\mathrm{s}$ pairs over one half $\bar{\mathrm{u}}\mathrm{u} + \bar{\mathrm{d}}\mathrm{d}$ pairs (the so-called Wroblewski ratio λ_S) turns out to be around 0.2-0.25 at all energies, whereas it is definitely higher in heavy ion collisions (see Fig. 11).

These differences, both in γ_S and λ_S have been and still are subject of investigation.

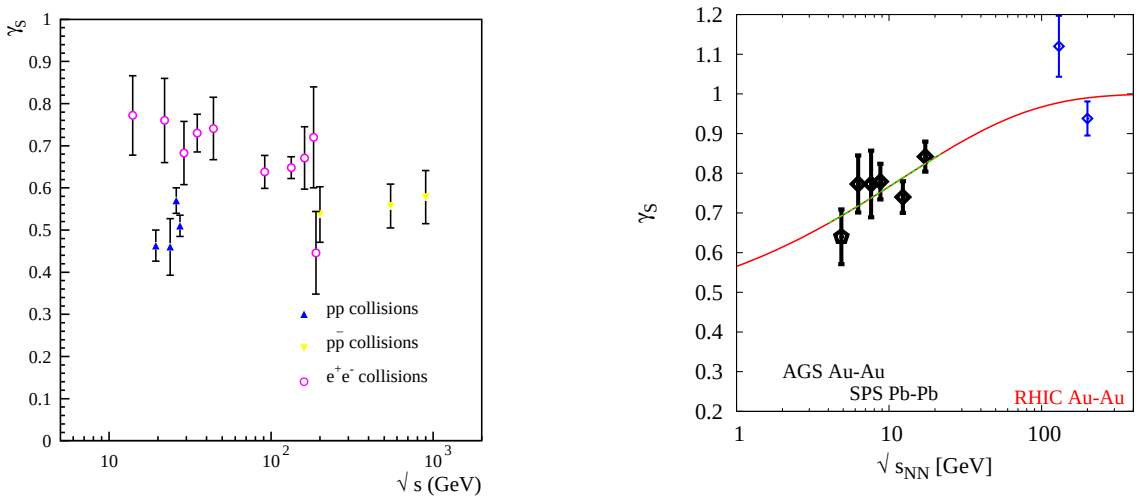

Figure 10: Left panel: the strangeness undersaturation parameter γ_S as a function of center-of-mass energy in e^+e^-, pp and $p\bar{p}$ collisions. Right panel: the strangeness undersaturation parameter γ_S as a function of center-of-mass energy in central heavy ion collisions (from ref. [23]).

Relevant information comes from the centrality dependence of strangeness production, which provides an interpolation from single pp collisions at large values of nuclear impact parameter to head-on heavy-ion collisions at low values thereof. The enhancement has been measured by the experiments WA97 and NA57 at SPS energy [27] and STAR at RHIC [28] for hyperons and other strange particles and it has been found to be hierarchical in strangeness content (highest for Ω^-, lowest for Λ). These observations led some authors [29] to put forward a picture where γ_S is an effective parametrization of a canonical suppression. For large enough baryon number and charge, it is possible to take a mixed canonical-grand-canonical approach where only strangeness conservation is enforced, while electric and baryon-chemical potential are introduced. The chemical factors $Z(S-S_j)/Z(S)$ depend on the volume and saturate at large volumes, as expected. Therefore, if we want to account for $\gamma_S < 1$ with this mechanism, there must be some small sub-regions within a large fireball where strangeness is exactly vanishing even for the most central collisions. Thereby, chemical factors are significantly less than 1 and a suppression with respect to the grand-canonical limit is implied. However, this model has two major problems:

1. Since measured enhancement steadily increases from peripheral to central collisions and hadronization temperature does not change [30, 31, 23], the volume of the sub-regions with $S = 0$ should also increase and a saturation is thus expected (see Fig. 12); yet, no saturation is observed, which is quite an oddity.

2. As has been mentioned, canonical suppression has no effect on ϕ; yet, the relative yield of this meson with two constituent strange quarks is also observed to increase

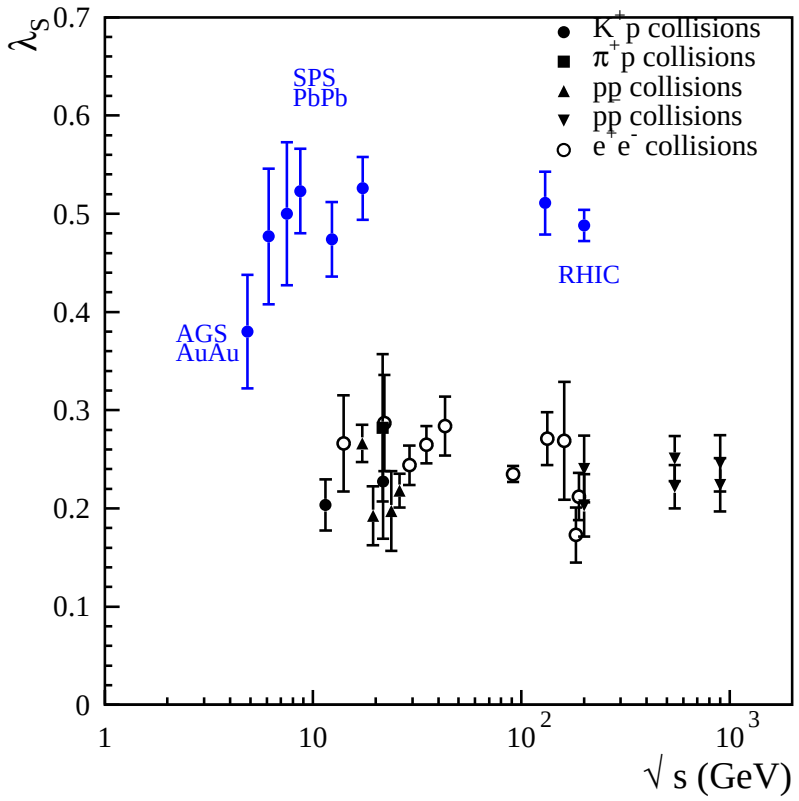

Figure 11: Wroblewski ratio λ_S (see text for definition) as determined in elementary and heavy ion collisions from fits of multiplicities to the statistical hadronization model.

from peripheral to central collisions [32] and with $\gamma_S = 1$ and the observed constant temperature, this cannot occur.

Recently, a geometrical explanation of these two features has been advocated [33] based on a superposition of emission from a hadron-resonance gas at full chemical equilibrium with $\gamma_S = 1$, defined as the *core*, and from nucleon-nucleon collisions at the boundary of the overlapping region of the two colliding nuclei, defined as the *corona*, from which produced particles escape unscathed. Since in NN collisions strangeness is suppressed with respect to a fully equilibrated, grand-canonical hadron gas, if such NN collisions account for a significant fraction of total particle production, a global fit to particle multiplicities will find $\gamma_S < 1$, as indeed observed in data. The idea of superposing different sources is common to other models (a similar one is discussed in ref. [34]). The peculiar feature of this specific model is to assume single NN collisions as secondary sources; only in this case does it seem possible to reproduce centrality dependence of the ϕ meson.

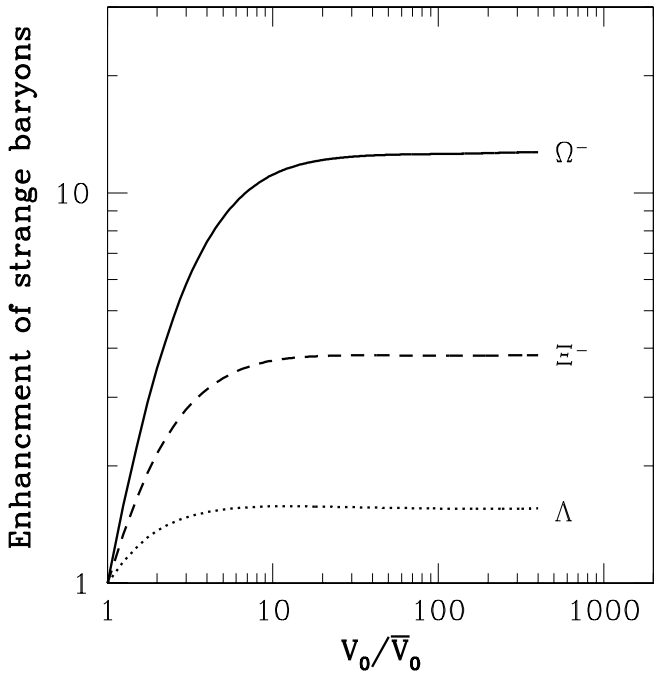

Figure 12: Canonical enhancement (defined here as the ratio between the chemical factor $Z(S - S_j)/Z(S)$ and its value at some fixed volume V_0) as a function of volume for hyperons (from ref. [29]).

10 Thermalization: how is it achieved?

After discussing the success of the SHM in reproducing particle multiplicities and the intriguing universality of its main parameter, the temperature, one is obviously led to the question how this can come about. A classical process of thermalization through binary collisions between formed hadrons, advocated in heavy ion collisions [35], is ruled out in elementary collisions because the expansion rate is fast and hadrons are not interacting for a long enough time for this to take place. But even in heavy ion collisions peculiar features of the data cannot be explained in a hadronic kinetic picture [36] without invoking the predominance of multi-body collisions; since, in this case, the hadronic mean free path is comparable or smaller than Compton wavelengths, the collisional picture breaks down naturally.

There is evidence that thermalization occurs at a relatively early stage over a large region (i.e. clusters several femtometers wide) in heavy ion collisions, whereas it is a late phenomenon (i.e. very close to hadronization) occurring over small (of the order of 1 fm) distances in elementary collisions. Yet, the agreement between model and data is surprisingly accurate in elementary collisions, even more accurate than in heavy ion collisions, the only difference being in the level of strangeness phase space saturation. Somehow, the hadrons must *be born into equilibrium* as Hagedorn first pointed out [37] and was reaffirmed by others [38, 39].

The idea that this thermal-like behavior is of genuine quantum-mechanical origin and not related to semi-classical collision processes, is shared by many [39] including the author. A different point of view was presented in ref. [40] where it was argued that the thermal behavior could just be *mimicked* by a matrix element which is weakly dependent on the final kinematic variables in (16), a scenario called "phase space dominance". But even this scenario requires stringent conditions on the dependence of cluster decay rates on the channel multiplicity (essentially like A^N) [10] such that the exponential dependence of production rates on mass is not spoiled. Hence phase-space dominance is not less trivial in any way. A possible path to distinguish between the two scenarios is provided by the analysis of exclusive rates at low energy, although it must be pointed out that the observed identical particle correlations already favors SHM which is endowed with a built-in spacial extension, unlike phase-space dominance.

However, whether it is a proper thermal-statistical equilibrium in a finite volume or rather a phase space dominance effect, there must be a profound reason behind this phenomenon, which ultimately has to be related to the nature of QCD as a theory with strong coupling at large distances. Also, we believe that the intriguing universality of the temperature found in elementary collisions as well as heavy ion collisions and its resemblance of the QCD critical temperature is not accidental.

If we assume that post-hadronization collisions are unable to restore equilibrium, how can a quantum evolution process ensure it? Several years ago it was pointed out that a closed quantum system whose classical counterpart is chaotic and ergodic can give rise to thermal distributions provided that the so-called Berry conjecture applies [41]. Berry's conjecture [42] essentially states that the high-lying eigenfunction amplitudes $\psi(\mathbf{x})$ in configuration space appear to be random Gaussian numbers and, as a consequence, momentum space distribution is microcanonical [43]. This "quantum thermalization" mechanism has been invoked to explain the observed thermal-like distributions in hadronic processes [44]. Of course, this argument requires that classical QCD is chaotic (as it has indeed been advocated [45]), that Berry's conjecture holds for quantum fields, and that it can be applied to a dynamical process like hadronization. All of these conditions are non-trivial, but pursuing these ideas further may give rise to interesting developments.

Recently, another appealing idea to explain the universality of thermal features in multihadron production has been put forward [46]. It invokes an analogy between confinement and black hole physics. It is conjectured that the phenomenon of confinement is equivalent to the formation of an event horizon for colored signals (quarks and gluons). Similarly to Hawking-Unruh radiation, the spectrum of hadrons, emitted as the result of a high energy collision, is thermal because no information can be conveyed from the causally disconnected region beyond event horizon. According to this so-called Hawking-Unruh scheme of hadronization, temperature is related to the string tension and is thereby universal. Another interesting consequence of this idea is that the extra strangeness suppression observed in elementary collisions can be quantitatively explained [17] as an effect of the different strange quark mass.

These attempts relating the observed thermal features in hadron production pro-

cesses to quantum chaos or Hawking-Unruh radiation are still in a developmental stage. Whether they will keep their promises will be seen in the future. Certainly, both share the vision that there is a fundamental quantum mechanical mechanism behind this phenomenon and no (or little) room for a classical collisional thermalization process.

11 Summary

The statistical model has been applied to a wide variety of small and large systems, spanning more than two orders of magnitude in center of mass energy $\sqrt{s}$ and revealing intriguing universal features of the hadronization process. The assumptions of the model were found to hold in a remarkable way for relative abundances and transverse momentum spectra of both light and heavy flavored species.

This model is based on few simple principles which seem to capture key universal features in the process of hadron formation. While this does not answer the central questions of confinement and chiral symmetry breaking, which are of fundamental importance for QCD, it certainly allows us to understand some of the key properties of QCD in the non-perturbative regime.

Acknowledgements

I would like to thank W. Alberico and M. Nardi for their warm hospitality and for their superb work in organizing this school. I am deeply grateful to R. Stock and R. Fries for their suggestions and invaluable help in improving the manuscript.

References

[1] E. Fermi, Prog. Th. Phys. **5** 570 (1950).

[2] R. Hagedorn, Nuovo Cim. Suppl. **3** 147 (1965).

[3] J. Cleymans, H. Satz, Z. Phys. C **57** 135 (1993); P. Braun-Munzinger, J. Stachel, J. P. Wessels and N. Xu, Phys. Lett. B **365** 1 (1996); F. Becattini, M. Gazdzicki and J. Sollfrank, Eur. Phys. J. C **5** 143 (1998); P. Braun-Munzinger, D. Magestro, K. Redlich and J. Stachel, Phys. Lett. B **518**, 41 (2001); A. Baran, W. Broniowski and W. Florkowski, Acta Phys. Polon. B **35** 779 (2004); J. Cleymans, B. Kampfer, M. Kaneta, S. Wheaton and N. Xu, Phys. Rev. C **71** 054901 (2005); F. Becattini, M. Gazdzicki, A. Keranen, J. Manninen and R. Stock, Phys. Rev. C **69** 024905 (2004);

[4] F. Becattini, Z. Phys. C **69** 485 (1996); F. Becattini and U. W. Heinz, Z. Phys. C **76** 269 (1997); F. Becattini and G. Passaleva, Eur. Phys. J. C **23** 551 (2002); F. Becattini, P. Castorina, J. Manninen and H. Satz, arXiv:0805.0964, to appear in Eur. Phys. J. C.

[5] G. Corcella et al, J. High En. Phys., 0101:010 (2001) and references therein.

[6] D. Amati and G. Veneziano, Phys. Lett. B **83**, 87 (1979).

[7] A. Chodos et al, Phys. Rev. D **9** 3471

[8] F. Becattini and L. Ferroni, Eur. Phys. J. C **51**, 899 (2007).

[9] F. Becattini and L. Ferroni, Eur. Phys. J. C **35**, 243 (2004).

[10] F. Becattini, J. Phys. Conf. Ser. **5**, 175 (2005).

[11] F. Becattini and L. Ferroni, Eur. Phys. J. C **52**, 597 (2007).

[12] M. Chaichian, R. Hagedorn, M. Hayashi, Nucl. Phys. B **92** 445 (1975).

[13] S. Weinberg, *The Quantum Theory Of Fields* Vol. 1 Cambridge University Press.

[14] R. Dashen, S. Ma, H. Bernstein Phys. Rev. **187** 345 (1969);
R. Dashen, R. Rajamaran, Phys. Rev. D **10** 694 (1974).

[15] F. Becattini and L. Ferroni, Eur. Phys. J. C **38**, 225 (2004).

[16] F. Becattini and G. Passaleva, Eur. Phys. J. C **23** 551 (2002).

[17] F. Becattini, P. Castorina, J. Manninen and H. Satz, Eur. Phys. J. C **56** 493 (2008).

[18] A. Keranen and F. Becattini, Phys. Rev. C **65**, 044901 (2002).

[19] J. Rafelski and M. Danos, Phys. Lett. B **97**, 279 (1980);
L. Turko, Phys. Lett. B **104**, 153 (1981);
R. Hagedorn and K. Redlich, Z. Phys. C **27**, 541 (1985);
S. Hamieh, K. Redlich and A. Tounsi, Phys. Lett. B **486**, 61 (2000)

[20] U. W. Heinz, arXiv:hep-ph/0407360.

[21] F. Becattini, M. Gazdzicki, A. Keranen, J. Manninen and R. Stock, Phys. Rev. C **69**, 024905 (2004).

[22] F. Becattini, M. Gazdzicki, J. Manninen, Phys. Rev. C **73**, 044905 (2006).

[23] J. Manninen, F. Becattini, arXiv:0806.4100, Phys. Rev. C in press.

[24] J. Rafelski and B. Muller, Phys. Rev. Lett. **48**, 1066 (1982).

[25] F. Becattini, M. Gazdzicki and J. Sollfrank, Eur. Phys. J. C **5** (1998) 143.

[26] J. Sollfrank, F. Becattini, K. Redlich and H. Satz, Nucl. Phys. A **638** (1998) 399C.

[27] F. Antinori et al., NA57 coll., J. Phys. G **32**, 427 (2006).

[28] B. I. Abelev *et al.*, STAR Collaboration, Phys. Rev. C **77**, 044908 (2008).

[29] S. Hamieh, K. Redlich and A. Tounsi, Phys. Lett. B **486** (2000) 61;

[30] J. Adams *et al.*, STAR Collaboration, Phys. Rev. Lett. **98** (2007) 062301.

[31] J. Cleymans, B. Kampfer, P. Steinberg and S. Wheaton, *Strangeness saturation: Energy and system-size dependence*, arXiv:hep-ph/0212335; J. Cleymans, B. Kampfer, M. Kaneta, S. Wheaton and N. Xu, Phys. Rev. C **71** 054901 (2005).

[32] B. I. Abelev *et al.*, STAR Collaboration, arXiv:0809.4737 [nucl-ex].

[33] F. Becattini and J. Manninen, J. Phys. G **35**, 104013 (2008); F. Becattini and J. Manninen, arXiv:0811.3766 [nucl-th].

[34] C. Hohne, F. Puhlhofer and R. Stock, Phys. Lett. B **640**, 96 (2006).

[35] P. Braun-Munzinger, J. Stachel and C. Wetterich, Phys. Lett. B **596**, 61 (2004); C. Greiner, P. Koch-Steinheimer, F. M. Liu, I. A. Shovkovy and H. Stoecker, J. Phys. G **31**, S725 (2005).

[36] U. Heinz and G. Kestin, PoS C **POD2006**, 038 (2006)

[37] R. Hagedorn, CERN lectures *Thermodynamics of strong interactions* (1970).

[38] F. Becattini and U. W. Heinz, Z. Phys. C **76** 269 (1997); U. Heinz, Nucl. Phys. A **661** 140 (1999).

[39] R. Stock, Phys. Lett. B **456** 277 (1999).

[40] J. Hormuzdiar, S. D. H. Hsu, G. Mahlon, Int. J. Mod. Phys. E **12** 649 (2003).

[41] M. Srednicki, Phys. Rev. E **50** 888 (1994).

[42] M. Berry, J. Phys. A **10** 2083 (1977).

[43] C. Jarzynski, Phys Rev E **56**, 2254 (1997).

[44] A. Krzywicki, arXiv:hep-ph/0204116.

[45] T. S. Biro, S. G. Matinyan and B. Muller, *Chaos and gauge field theory*, World Sci. Lect. Notes Phys. **56**, 1 (1994); R. Pullirsch, K. Rabitsch, T. Wettig and H. Markum, Phys. Lett. B **427**, 119 (1998).

[46] P. Castorina, D. Kharzeev and H. Satz, Eur. Phys. J. C **52**, 187 (2007).